J BONE ONCOL 47 (2024) 100616

Contents lists available at ScienceDirect

Journal of Bone Oncology

journal homepage: www.elsevier.com/locate/jbo

Research Paper

Impact of quantitative CT texture analysis on the outcome of CT-guided bone biopsy

Silvio Wermelskirchen [a,1], Jakob Leonhardi [a,1], Anne-Kathrin Höhn [b], Georg Osterhoff [c], Nikolas Schopow [c], Silke Zimmermann [d], Sebastian Ebel [a], Gordian Prasse [a], Jeanette Henkelmann [a], Timm Denecke [a], Hans-Jonas Meyer [a,*]

[a] Department of Diagnostic and Interventional Radiology, University of Leipzig, Leipzig, Germany
[b] Department of Pathology, University Hospital Leipzig, University of Leipzig, Germany
[c] Department of Department of Orthopaedics, Trauma and Reconstructive Surgery, University Hospital Leipzig, Germany
[d] Institute of Laboratory Medicine, Clinical Chemistry and Molecular Diagnostics, University of Leipzig, Leipzig, Germany

HIGHLIGHTS

- CT texture analysis can aid to predict an unsuccessful biopsy result.
- The prediction model reached an AUC of 0.80.
- Relevant biopsy results are identified between osteolytic and osteoblastic lesions.

ARTICLE INFO

Keywords:
CT
Bone biopsy
Texture analysis

ABSTRACT

Texture analysis can provide new imaging-based biomarkers. Texture analysis derived from computed tomography (CT) might be able to better characterize patients undergoing CT-guided percutaneous bone biopsy. The present study evaluated this and correlated texture features with bioptic outcome in patients undergoing CT-guided bone biopsy. Overall, 123 patients (89 female patients, 72.4 %) were included into the present study. All patients underwent CT-guided percutaneous bone biopsy with an 11 Gauge coaxial needle. Clinical parameters and quantitative imaging features were investigated. Random forest classifier was used to predict a positive biopsy result. Overall, 69 patients had osteolytic metastasis (56.1 %) and 54 had osteoblastic metastasis (43.9 %). The overall positive biopsy rate was 72 %. The developed radiomics model demonstrated a prediction accuracy of a positive biopsy result with an AUC of 0.75 [95 %CI 0.65 – 0.85]. In a subgroup of breast cancer patients, the model achieved an AUC of 0.85 [95 %CI 0.73 – 0.96]. In the subgroup of non-breast cancer patients, the signature achieved an AUC of 0.80 [95 %CI 0.60 – 0.99]. Quantitative CT imaging findings comprised of conventional and texture features can aid to predict the bioptic result of CT-guided bone biopsies. The developed radiomics signature aids in clinical decision-making, and could identify patients at risk for a negative biopsy.

1. Introduction

Adequate histologic tissue sampling is of great importance in oncological patients [1,2]. At the present, computed tomography (CT)-guided percutaneous core needle biopsy (CNB) has widely been established as the standard for sampling and assessing suspected bone metastasis [3–6], as CT guidance is beneficial in both reducing accidental trauma to adjacent organs and neurovascular structures, as well as in the confirmation of correct regional sampling [7,8].

The current literature states conflicting results of the diagnostic yield achieved by CT-guided percutaneous CNB of a suspected bone lesion, with estimates ranging between 69–87.4 % [4,5,9], mainly depending on lesion characteristics such as presence and degree of sclerosis as well as the lesion diameter. Moreover, the biopsy outcome for lytic lesions is

Abbreviations: CT, computed tomography; ROC, receiver operating characteristics-curve; AUC, area under the curve; ROI, region of interest; HU, Hounsfield unit.

* Corresponding author at: Department of Diagnostic and Interventional Radiology, University of Leipzig, Germany.
E-mail address: Hans-jonas.meyer@medizin.uni-leipzig.de (H.-J. Meyer).

[1] These authors contribute equally for this work.

https://doi.org/10.1016/j.jbo.2024.100616
Received 14 January 2024; Received in revised form 14 June 2024; Accepted 14 June 2024
Available online 19 June 2024

better investigated and was superior compared to osteoblastic lesions [5,11,12].

In the clinical setting, adequate bioptic targeting of sclerotic lesions present a challenging task because of the increased likelihood of negative results and the often-minuscule yield of malignant cells, which may additionally prevent a further in-depth histopathological characterization of the probe [1,5,13]. This is noteworthy, as up to half of the patients with highly prevalent cancers, such as prostate and breast cancer, present exclusively with skeletal manifestations of the disease, which could impose difficulties for diagnosis [14–16]. Therefore, acquiring viable histological proof of malignancy is of critical importance and correct localization for tissue sampling could enhance the outcome of the biopsy. Up to now, few investigations have addressed possible influencing factors between both interventional as well as lesion characteristics and diagnostic yield [4,5,11]. Lytic lesions, larger lesions and longer specimens are relevant factors for a positive biopsy outcome [11].

With the emergence of texture analysis research, novel biomarkers derived from radiological images can be used for additional quantitative image assessment [17–22]. Various texture analysis applications have been described in the literature, with its main focus being centered on further enhancing oncological decision-making [17–23]. Different spatial characteristics were used for better discrimination purposes, treatment prediction, and prognosis stratification in several tumor entities. In short, texture analysis derived from radiological images can provide quantitative information beyond the radiologist's clinical observation scope. This could be of great clinical importance to further analyze the preinterventional images and to stratify patients, who could benefit from the CT-guided intervention and those, who could not.

However, to date, no study has investigated the diagnostic potential of texture analysis to predict the outcome of bone biopsies.

In light of the critical importance of identifying malignant bone lesions not only in the initial diagnosis of a disease but also in the treatment and follow-up of patients, texture analysis of potential biopsy sides seems of particular clinical interest and relevance. Quantitative imaging should aid in the complex clinical decision-making process in patients with possible bone metastasis.

Therefore, the purpose of the present study was to investigate whether CT-derived texture analysis parameters, as well as interventional and lesion characteristics, can improve the diagnostic performance for bone biopsy sampling.

2. Material and methods

2.1. Patient acquisition

This retrospective study was approved by the institutional review board (University hospital of Leipzig, register no. 344–2007).

All patients with a CT-guided bone biopsy were retrospectively assessed within the period 2018 to 2022. Inclusion criteria were available CT images, sufficient histopathology results, and detectable lesion on CT images. Exclusion criteria were severe imaging artifacts, e.g. due to metal implants.

Overall, 123 patients (89 female patients, 72.4 %) were included into the present study. The median age at the time of CT acquisition was 65.6 years (IQR 20 years), ranging from 37 to 91 years. The primary tumors were comprised of 70 patients with breast cancer (56.9 %), followed by 8 patients with lung cancer (6.5 %) and 7 patients with prostate cancer (5.9 %). Other primary cancers were rare. 73 lesions were located within the pelvis (59.3 %), followed by 43 lesions were located within the spine (35.0) and 7 lesions within the sternum (5.7 %).

2.2. Interventional procedure

Written informed consent for CT-guided biopsy was obtained from each patient before the intervention. The biopsies were performed by five interventional radiologists having more than five years of experience in interventional radiology. Pre-procedure complete blood count and coagulation profile were obtained. The biopsy was performed with platelet count of at least 50.000/mm^3, prothrombin time $>$ 50 %, and partial thromboplastin time $\leq$ 1.5 times. The alkaline phosphatase (AP) and lactate dehydrogenase (LDH) were extracted from the last blood sample before biopsy.

Before beginning the procedure, the interventional strategy, especially the patient's position and biopsy pathway were planned using pre-biopsy CT images. The intervention was started with skin disinfection, and subcutaneous local anesthesia advanced toward the planned pathway using 10–20 ml lidocaine 1 % (Xylocitin, Jenapharm, Germany). The biopsy was performed using a coaxial 11 Gauge biopsy system. The corticalis penetration was performed manually and then an automatic driller was used to guide and penetrate the needle throughout the suspicious bone lesion. Procedural CT acquisitions were measured to assess whether the needle tip properly reached the target lesion. After needle removal, post-biopsy CT images were acquired to detect complications, especially hematoma.

2.3. Imaging technique

All CT-guided bone biopsies were performed on the same 16-slice CT scanner (Brilliance Big Bore, Philips, Hamburg, Germany). Typical imaging parameters were: 100 kVp; 125 mAs; slice thickness, 1 mm; pitch, 0.9. CT scanner. A conventional CT scan of the region of interest without contrast media application was obtained prior to the intervention and was used to plan the best way to access the lesion.

2.4. Conventional imaging analysis

Osteolytic metastasis was defined as a structural hypodense defect within the bone, either with a clear or irregular border. Osteoblastic metastasis was defined as a hyperdense lesion of the bone ranging from slight hyperdense to strong hyperdense.

The biopsy tract's needle length, angle, and HU units were measured on the pre-interventional planning CT scan. Biopsy tract distance was obtained by assessing the tract's distance upon entering the patient's skin to the deepest osseus penetration of the biopsy needle. In addition, the distance between the cortical entrance of the biopsy needle till the deepest osseous penetration along the biopsied path was obtained. Furthermore, the osseous biopsy tracts HU were determined by drawing a region of interest (ROI) on the pre-interventional scan along the path of the biopsy tract as determined by the following interventional CT scans. As reported by Donners et al., a cut-off value of 610 HU can be used to predict osteoblastic lesions with a worse biopsy outcome [24]. This threshold value was used to divide the osteoblastic lesions.

The angle was measured by using the deepest osseous needle penetration as the vertex, the biopsy tract as one arm of the angle, and the shortest channel perpendicular to the plane of the skin as the other arm.

2.5. Texture analysis

CT images analyzed with the texture analysis software MaZda (version 4.7, available at http://www.eletel.p.lodz.pl/mazda/) [25,26]. A polygonal ROI was placed on the largest representative slide of the bone metastasis on the largest, proximal position. The ROI was clearly drawn in accordance to the following biopsy tract of the biopsy needle. The measurements were performed in a blinded manner to the clinical results by a resident of radiology with four years of general experience (J.L.) For each ROI, gray-level (μ) normalization was performed, using the limitation of dynamics to $\mu \pm 3$ standard deviations to minimize the influence of contrast and brightness variation, as it was performed in similar studies utilizing texture analysis [27].

Altogether, 279 first and second order texture features were retrieved for every patient. The robustness of the texture feature extraction for MaZda was demonstrated previously and was comparable

to the extraction performed by PyRadiomics [28]. The performed analysis therefore adheres to the proposed Image Biomarker Standardisation Initiative [29].

Fig. 1 displays a representative case of the patient sample for illustration purposes.

2.6. Texture feature cleansing and selection

A Spearman's correlation matrix analysis was performed using R (version 3.5.1) to reduce possible multicollinearity. Firstly, highly correlated texture features with correlation coefficient larger than r = 0.7 were removed in order to avoid weakening of the regression model. Secondly, the texture features were further evaluated with the random forest (RF) model, ranking the features according to their importance to the model. RF is an ensemble model that consists of multiple decision trees, each fitted to a random subset of the input data. The probability of class membership is determined by the majority vote in the ensemble [30]. Based on the ranking results, we fitted the features in forward regression analysis, extracting the feature signature, which was able to predict the biopsy outcome.

2.7. Histopathology analysis

After the biopsy cores were obtained, they were fixed for 24–30 h and decalcified in an Ethylenediaminetetraacetic acid solution for two days. Tumor content was assessed by an experienced pathologist during clinical work-up. Histopathology success was deemed as non-diagnostic or diagnostic according to need for re-biopsy. Every negative biopsy result was secured as malignant in re-biopsy or during clinical work-up. The patient groups were stratified accordingly to the primary tumor.

2.8. Statistical analysis

The statistical analysis and graphics creation were performed using GraphPad Prism 6 (GraphPad Software, La Jolla, CA, USA) and SPSS (IBM, Version 25.0; Armonk, NY, USA). Collected data were evaluated by means of descriptive statistics (absolute and relative frequencies). Spearman's correlation coefficient (r) was used to analyze associations between investigated scores after testing for normality distribution. Group differences were calculated with Mann-Whitney-*U* test and Fisher's exact test when suitable. Diagnostic accuracy was further investigated by receiver operating characteristics-curve (ROC) with reported area under the curve (AUC). In all instances, p-values < 0.05 were taken to indicate statistical significance.

3. Results

Of the 123 analyzed metastasis, 69 patients had osteolytic metastasis (56.1 %) and 54 patients had osteoblastic metastasis (43.9 %).

The overall tumor positive rate of the performed biopsies was 86 of 123 cases (72 %).

The clinical and imaging features are shown in Table 1.

In breast cancer patients, the length of the skin to lesion was statistically significant longer compared to non-breast cancer patients (86.88 ± 21.28 mm versus 74.39 ± 20.44 mm, p = 0.0016). Moreover, the biopsy tract angle was slightly higher in non-breast cancer patients (32.47 ± 64.30° versus 32.17 ± 20.36°, p = 0.02). In the assessment of serum parameters, the AP was higher in non-breast cancer patients (4.27 ± 8.67 μkat/l versus 2.02 ± 1.53 μkat/l, p = 0.03) compared to breast cancer patients.

Table 2 provides the clinical and interventional features in accordance to the metastasis type. The overall positive biopsy rate was higher in osteolytic metastasis compared to osteoblastic (n = 55 of 69, 82 %

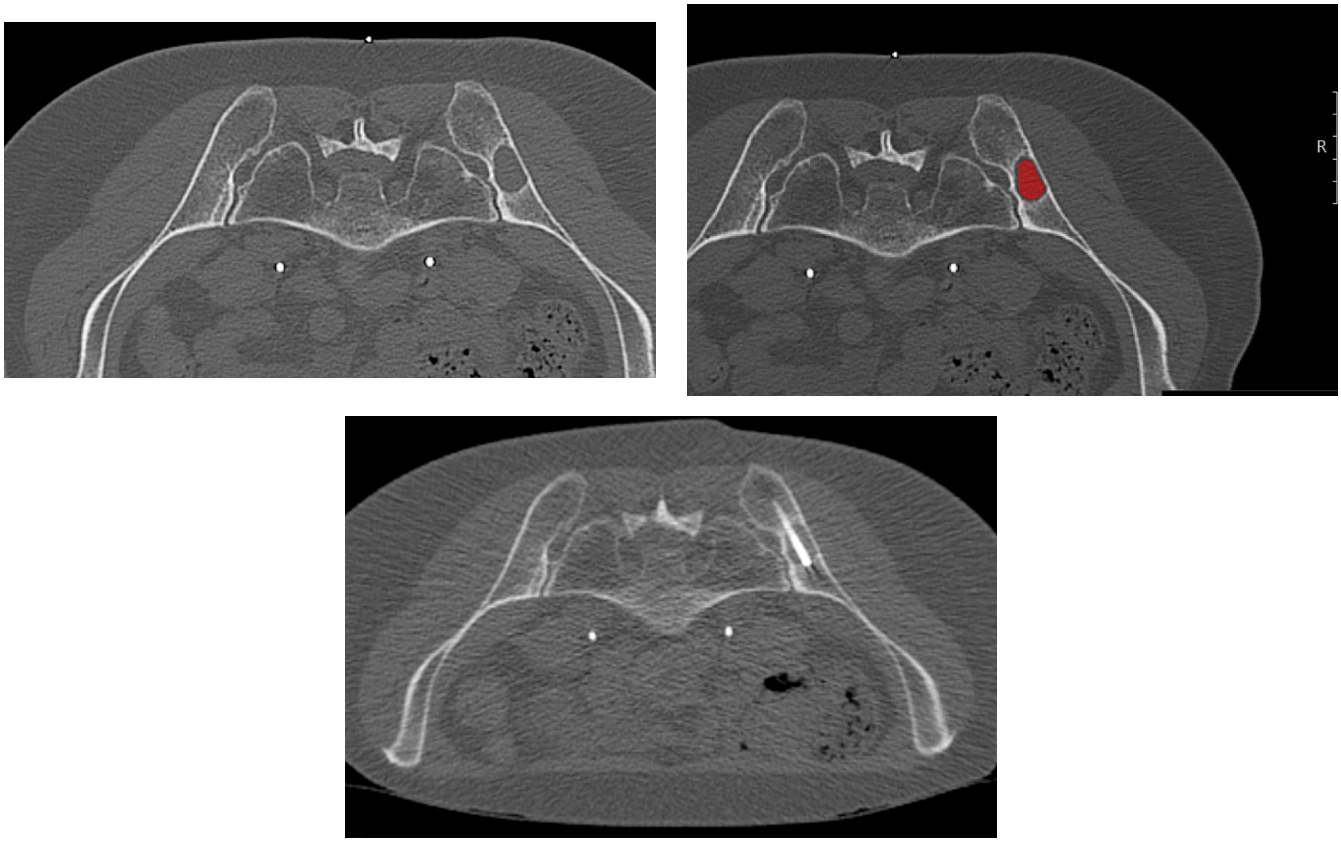

Fig. 1. A. A representative case of the patient sample with an osteolytic metastasis within the right iliac bone in a female patient with cervical cancer. **B.** The region of interest was drawn within the boundary of the lesion. **C.** The biopsy needle was penetrated through the lesion.

Table 1
Demographic overview of the patient sample.

Clinical and puncture feature	breast cancer (n = 70)	non breast cancer (n = 53)	p-value
Gender (female) N=, %	70 (97 %)	19 (37 %)	**0.00001**
Biopsy (+) N=, %	55 (76 %)	31 (63 %)	0.15
Osteolytic metastasis N=, %	36 (50 %)	32 (64 %)	0.14
Age (years)	64.1 ± 12.2	67.6 ± 13.6	0.07
lesion HU	340.47 ± 289.72	251.03 ± 247.66	0.09
longest lesion diameter	23.38 ± 13.99	25.75 ± 16.15	0.43
shortest lesion diameter	15 ± 7.38	16.84 ± 8.27	0.29
biopsy tract HU	305.15 ± 188.86	258.18 ± 212.34	0.06
biopsy tract length skin to lesion in mm	86.88 ± 21.28	74.39 ± 20.44	**0.0016**
biopsy tract bone to lesion in mm	29.23 ± 14.87	31.82 ± 16.48	0.52
biopsy tract angle in °	32.17 ± 20.36	32.47 ± 64.30	**0.02**
AP µkat/l	2.02 ± 1.53	4.27 ± 8.67	**0.03**
LDH µkat/l	4.49 ± 0.98	5.26 ± 2.56	0.98
Hb mmol/l	7.77 ± 1.05	7.62 ± 1.27	0.35
platelets exp 9/l	252.24 ± 84.84	263.68 ± 134.1	0.97

Table 2
Comparison between patients with osteolytic and osteoblastic metastasis.

Clinical and puncture feature	Osteolytic (n = 69)	Osteoblastic (n = 54)	p-value
Gender (female) N=, %	46 (67 %)	43 (80 %)	0.16
Biopsy (+) N=, %	55 (82 %)	31 (57 %)	**0.0044**
breast cancer N=, %	36 (52 %)	36 67 %)	0.14
Age (yrs)	65.36 ± 13.26	65.80 ± 12.46	0.97
lesion HU	95.41 ± 60.54	569 ± 204.55	**0.0001**
longest lesion diameter	28.26 ± 17.56	19.39 ± 8.43	**0.0018**
shortest lesion diameter	17.97 ± 8.57	12.94 ± 5.55	**0.0005**
biopsy tract HU	168 ± 112.41	435.87 ± 184.63	**0.0001**
biopsy tract length skin to lesion in mm	80.23 ± 23.09	83.59 ± 19.94	0.40
biopsy tract bone to lesion in mm	31.69 ± 16.45	28.53 ± 14.27	0.28
biopsy tract angle in °	28.18 ± 19.62	37.56 ± 62.54	0.65
AP µkat/l	3.46 ± 7.16	2.07 ± 1.58	0.05
LDH µkat/l	4.72 ± 2.05	4.85 ± 1.33	0.33
Hb mmol/l	7.69 ± 1.22	7.73 ± 1.05	0.92
platelets exp 9/l	256.76 ± 101.86	257.22 ± 115.25	0.51

versus n = 31 of 54, 57 %, p = 0.004). The osteolytic lesions were statistically significant larger (28.26 ± 17.56 mm versus 19.39 ± 8.43 mm, p = 0.0018).

In a further analysis, the groups were investigated accordingly to the biopsy results, which is summarized in Table 3. The previously proposed threshold value of 610 HU was in 75 of 86 of cases (88 %) identified in the positive biopsy group, whereas it was present in 24 of 37 of cases (66 %) in the negative groups present (p = 0.0001). The longest diameter was also associated with the biopsy result. In the positive biopsy group the lesion was larger with 26.37 ± 16.56 mm, whereas in the negative group it was 19.32 ± 7.68 mm (p = 0.04). The mean HU of the lesion was lower in the positive biopsy group (254.60 ± 254.99 HU versus

Table 3
Comparison between patients with a positive and negative biopsy result.

Clinical and puncture feature	Positive biopsy result (n = 70)	Negative biopsy result (n = 53)	p-value
gender (female) N=, %	64 (73 %)	25 (71 %)	0.54
osteolytic N=, %	56 (65 %)	12 (34 %)	**0.02**
breast cancer N=, %	55 (63 %)	17 (49 %)	0.16
threshold < 610HU, N=, %	77 (88 %)	23 (66 %)	**0.00001**
Lesion diameter > 3 cm, N=, %	25 (28 %)	2 (6 %)	**0.007**
Age (yrs)	65.55 ± 13.27	65.57 ± 14.12	0.90
lesion HU	254.60 ± 254.99	426.06 ± 290.63	**0.003**
longest lesion diameter	26.37 ± 16.56	19.32 ± 7.68	**0.04**
shortest lesion diameter	16.51 ± 8.34	13.90 ± 5.87	0.15
biopsy tract HU	252.97 ± 180.39	367.91 ± 223.01	**0.01**
biopsy tract length skin to lesion in mm	81.21 ± 21.59	82.95 ± 22.39	0.62
biopsy tract bone to lesion in mm	31.84 ± 15.65	26.43 ± 14.81	0.06
biopsy tract angle °	27.52 ± 18.05	44.31 ± 76.85	0.21
AP µkat/l	3.29 ± 6.47	1.81 ± 1.37	0.05
LDH µkat/l	4.83 ± 1.79	4,6 ± 1.66	0.67
Hb mmol/l	7.66 ± 1.15	7.83 ± 1.14	0.43
platelets exp 9/l	253.38 ± 102.10	265.77 ± 121.14	0.75

426.06 ± 290.63 HU, p = 0.003). Tables 4(a-e) provides the statistically significant texture features of these group comparisons. Histogram-based percentile parameters were statistically significant different in every group comparison.

4. Diagnostic accuracy of texture features

The random forest classifier was used to predict the biopsy outcome. The model demonstrated a prediction accuracy of a positive biopsy result with an AUC of 0.75 [95 %CI 0.65 – 0.85]. The used parameters for the prediction model are biopsy tract HU, the second order texture features “S(1,1)Contrast”, “S(3,3)SumOfSqs”, “S(0,1)DifEntrp” and the area of the ROI. The second order texture features reflect the heterogeneity of the lesion and quantify the spatial appearances of the voxels with the resulting HU values in different manners. The corresponding graph is displayed in Fig. 2**a**.

Furthermore, a signature was used to predict the biopsy results in the subgroup of patients with breast cancer. The model demonstrated a prediction accuracy of positive biopsies with an AUC of 0.85 [95 %CI 0.73 – 0.96] (Fig. 2**b**). This signature is using the second order texture features “S(1,0)DifVarnc”, “S(0,4)DifEntrp”, “S(3,3)InvDfMom” and the

Table 4a
Comparison of the investigated texture features in accordance to the biopsy result.

Imaging and texture features	Negative biopsy result	positive biopsy result	p-value
_MinNorm	81.69 ± 41.18	61.45 ± 32.22	0.03
_MaxNorm	179.63 ± 64.01	143 ± 50.51	0.003
Mean	131.17 ± 42.95	102.78 ± 31.96	0.0006
Perc,01 %	94.57 ± 37.28	71.85 ± 27.99	0.007
Perc,10 %	110.77 ± 38.10	84.57 ± 30.25	0.0002
Perc,50 %	130.91 ± 43.56	102.78 ± 32 ± 53	0.0008
Perc,90 %	152.37 ± 50.78	119.78 ± 38.35	0.002
Perc,99 %	169.06 ± 56.59	113.95 ± 41.83	0.002
Sigma	0.27 ± 0.12	0.34 ± 0.17	0.04

Table 4b
Comparison of the investigated texture features in accordance to the biopsy result in a subanalysis of breast cancer patients.

Imaging and texture features	Negative biopsy result	positive biopsy result	p-value
_MinNorm	91 ± 39.69	64.78 ± 30	0.02
_MaxNorm	192.58 ± 63.20	148.11 ± 50.09	0.009
Mean	142.27 ± 42.70	106.94 ± 33.20	0.003
Perc.01 %	101.71 ± 37.25	75.11 ± 26	0.02
Perc.10 %	120.71 ± 37.63	89.07 ± 29.27	0.002
Perc.50 %	142.41 ± 43.33	106.84 ± 34.01	0.003
Perc90%	163.59 ± 49.86	124.67 ± 38.80	0.004
Perc.99 %	178.59 ± 53.93	138.73 42.14	0.006
Teta2	−0.72 ± 0.13	−0.64 ± 0.14	0.02
WaveEnLL_s-3	14352.31 ± 5412.67	17491.20 ± 4625.25	0.01
WavEnHL_s-3	520.20 ± 344.58	338.28 ± 327.92	0.01
WavEnLL_s-4	11328.17 ± 8268.5	18331.95 ± 8110.33	0.002

Table 4c
Comparison of the investigated texture features in accordance to the biopsy result in a subanalysis of all non-breast cancer patients.

Imaging and texture features	Negative biopsy result	positive biopsy result	p-value
_Mean	120.69 ± 41.64	95.85 ± 28.96	0.03
Perc.10 %	101.61 ± 37.25	77.06 ± 30.81	0.01
Perc.50 %	120.06 ± 42.08	96.03 ± 29.13	0.04
S(3,3)Correlat	0.18 ± 0.27	0.04 ± 0.24	0.03
S(3,3)SumVarnc	250.30 ± 64.37	214.24 ± 42.66	0.02
S(4,4)Contrast	183.28 ± 55.01	209.17 ± 54.52	0.03
S(4,4)Correlat	0.14 ± 0.26	0.00 ± 0.20	0.008
S(4,4)SumVarnc	243.41 ± 60.66	204.82 ± 39.07	0.003

Table 4d
Comparison of the investigated texture features in accordance to the biopsy result in a subanalysis of all osteoblastic metastasis.

Imaging and texture features	Negative biopsy result	positive biopsy result	p-value
_MaxNorm	209.74 ± 52.66	186 ± 52.41	0.03
Perc.90 %	176.74 ± 40.14	157.32 ± 38.75	0.02
Perc.99 %	196.04 ± 45.80	170.77 ± 40.01	0.01
S(0.5)DifVarnc	59.08 ± 20.44	47.23 ± 16.27	0.02

Table 4e
Comparison of the investigated texture features in accordance to the biopsy result in a subanalysis of all osteolytic metastasis.

Imaging and texture features	Negative biopsy result	positive biopsy result	p-value
S(5.-5)SumAverg	63.52 ± 2.39	63.72 ± 2.90	0.03
Teta4	0.05 ± 0.09	−0.02 ± 0.12	0.04
WavEnHL_s-3	350.78 ± 210.58	229.08 ± 188	0.02
WavEnHL_s-4	485.41 ± 279.31	263.90 ± 289.42	0.005
WavEnHH_s-4	213.53 ± 144.01	106.46 ± 99.22	0.01

histogram parameter "Perc,50 %". The histogram parameters represents the median HU value of the lesion and the second order texture features the heterogeneity of the lesion.

In the subgroup of non-breast cancer patients, the signature achieved an AUC of 0.80 [95 %CI 0.60 – 0.99] (Fig. 2**c**). This signature is using only two second order texture features "S(0,1)DifVarnc" and "S(0,1) SumOfSqs".

Further subgroup analyses were performed in regard of osteolytic or osteoblastic lesion. The model for osteoblastic lesions demonstrated a prediction accuracy with an AUC of 0.70 [95 %CI 0.54 – 0.86] (Fig. 2**d**). This signature is using three second order texture features "S(0,4) DifVarnc", "S(0,1)SumVarnc" and "S(3,3)SumOfSqs". For osteolytic lesions the model achieved an AUC of 0.66 [95 %CI 0.51 – 0.80] using three second order texture features "S(2,-2)SumAverg", "S(1,1) Contrast" and "S(1,-1)Entropy". The corresponding graph is displayed in Fig. 2**e**.

5. Discussion

The present study evaluated the diagnostic benefit of CT texture analysis and clinical parameters to predict the successful outcome of CT-guided osseous tumor biopsy.

As a key finding, we could demonstrate that CT texture features are different in accordance to the biopsy outcome. This could aid in clinical work up to better stratify patients, which could benefit of the biopsy and those with a deemed negative result.

Only a very limited number of studies sought to examine possible associations of imaging and clinical data with the outcome results of bone biopsies.

Texture analysis could enable a better tissue characterization based upon spatial differences of the CT images [17–20]. This was already further elucidated that CT texture analysis could provide insights into the biological behavior of tumors [17–20,28]. Presumably, this analysis could also provide novel considerations into the work-up of interventional radiologists for better planning of the CT-guided interventions.

Notably, the combined models employing clinical and CT texture features showed the highest accuracy to predict a negative biopsy result. This highlights the additive value of both the clinical information and the texture-based information of the target lesion.

As identified important texture features were the histogram-based percentile parameters predictors for outcome in almost every tumor subgroup analysis. Interestingly, there were low percentile values of 1 % in the overall analysis and breast cancer subgroup analysis, whereas for the non-breast cancer analysis 10 and 50 % were of importance.

The histogram parameters represent the distribution of HU values of the lesion within the histogram [23].

As another finding, there were distinctive differences within the second-order texture features between the breast cancer and non-breast cancer subgroup. In the breast cancer group, there were significant differences for the Wavelet analysis features, whereas for the non-breast cancer group there were differences identified for texture features derived from gray-level co-occurrence matrix [17–19]. These features reflect the spatial relationships of the different HU values of the lesions in different mathematical manners.

This is also an expression for the distinctive differences of the tumor composition between the different primary tumors and the resulting differences of the imaging phenotype.

One can assume that CT histogram values can reflect differences of the tumor composition of the target lesion and therefore can also aid in the correct localization for the biopsy.

As expected, for the osteoblastic lesions, the most important CT parameters were percentile based of 90 % and 99 % of the HU values. One can acknowledge that for the very dense lesions slight differences of the histogram in the high HU region can be reflected with these parameters and can indicate a possible negative biopsy result. This important finding could be used in patients with only osteoblastic lesions to identify a possible target lesion with a more favorable histogram value and therefore higher positive biopsy outcome.

One important aspect of every radiomics analysis is the robustness and generalization of the extracted imaging features [29]. The used MaZda package is a widely used texture feature software. Moreover, it was demonstrated that the extracted features are good comparable and robust compared to another widely used package PyRadiomics [28]. Another important point is that the most significant features in the present study were derived from the first order histogram group, which are more robust throughout different sites and vendors [31].

The overall tumor-positive biopsy rate of 72 % in our study is within

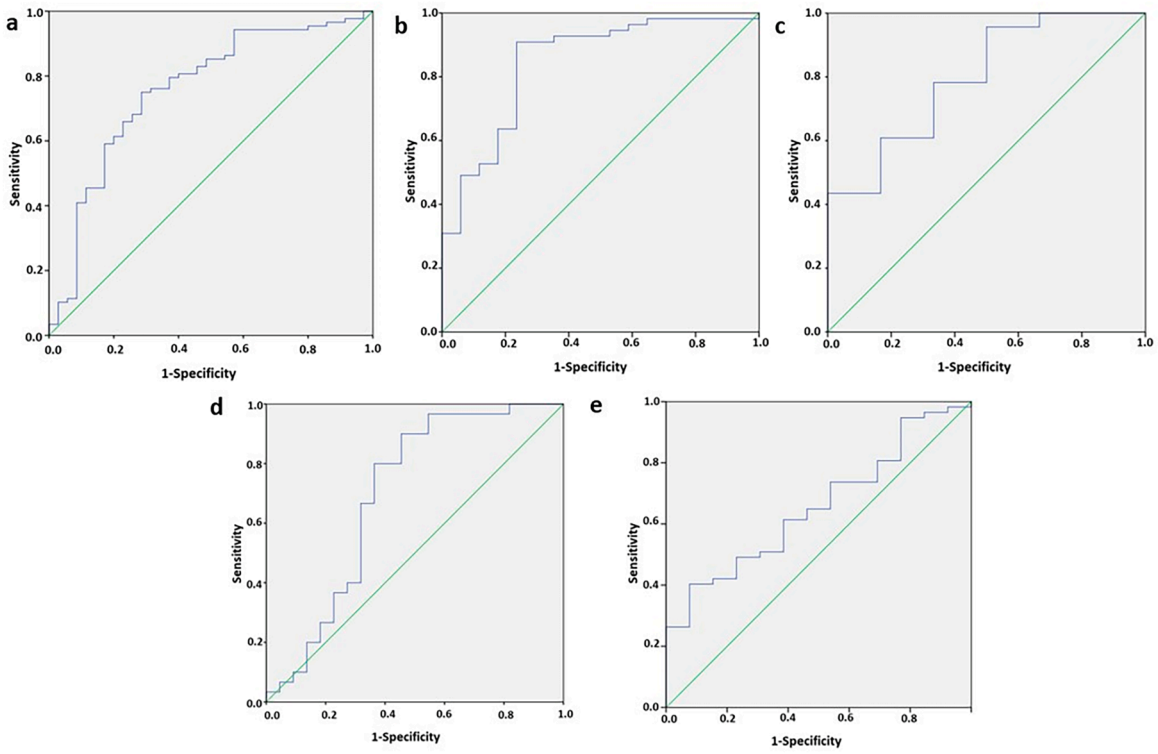

Fig. 2. A. Receiver operating characteristics-curve to predict a positive biopsy result in the overall cohort. The model demonstrated a prediction accuracy of a positive biopsy result with an AUC of 0.75 [95 %CI 0.65 – 0.85]. **b.** The subgroup analysis of breast cancer patients. The model demonstrated a prediction accuracy of positive biopsies with an AUC of 0.85 [95 %CI 0.73 – 0.96]. **c.** The subgroup analysis of non-breast-cancer patients. The signature achieved an AUC of 0.80 [95 %CI 0.60 – 0.99]. **d.** The subgroup analysis of osteoblastic metastasis. The model achieved an AUC of 0.70 [95 %CI 0.54 – 0.86]. **e.** The subgroup analysis of osteolytic metastasis. The model achieved an AUC of 0.66 [95 %CI 0.51 – 0.80].

the pooled frequency of 62–82 %, which was published in a meta analysis of 13 studies analyzing only sclerotic bone biopsies [13]. Better results were even published by Leffler et al. with a positive biopsy results in 82 % of cases and a negative predictive value of 100 % [32]. The positive rate of 57 % of the osteoblastic lesions of the present study is on the overall lower side of the published spectrum.

The present higher positivity rate for osteolytic lesions compared to sclerotic lesions is a common finding in the literature [10,33–35]. That is why, sclerotic/osteoblastic lesions are considered more challenging in clinical routine.

Conventional CT imaging findings were also previously investigated by some studies including lesion-to-cortex distance, skin-to-lesion distance, tract length, and number of cores obtained [4,10,24,33–35]. The novel texture parameters could be added into these known factors and, as it was shown in the present study, provide more insight into the microstructure of the target lesion.

There is definite need to evaluate the present results in a prospective study, whether it could change the interventionalist's decision for the target lesion and whether it could enhance the outcome of the CT-guided bone biopsy.

There are some limitations of the present analysis to address. First, it is a retrospective study with known inherent bias. Yet, the imaging analysis was performed blinded to the clinical and pathological results. Second, the patient sample is rather small with consequently small subgroup analyses. Third, although in all cases an 11G needle was used, the needle length and the extracted bone biopsy variated slightly and could have an influence on the biopsy result. Forth, only metastases were analyzed in the present study. It remains unclear, whether texture analysis could also aid in bone biopsy planning for primary tumors. Moreover, the study sample has a high frequency of breast cancer patients, which needs to be considered for generalization purposes. Fifth, the measurements were performed by one reader, which could lead to certain reader bias for the extraction of the CT texture features. However, the target lesions were clearly delineated along the following biopsy tract, which should lead to similar results, when performed by different experienced readers.

6. Conclusion

Quantitative CT imaging findings comprised of conventional and texture features can aid to predict the bioptic result of CT-guided bone biopsies. The developed radiomics signature might aid in clinical decision making, and could identify patients at risk for a negative biopsy.

7. Declarations

Institutional Review Board approval was obtained University hospital of Leipzig, register no. 344–2007.

Written informed consent was waived due to the retrospective study design.

8. Availability of data and materials

The datasets used and/or analyzed during the current study are available from the corresponding author on reasonable request.

CRediT authorship contribution statement

Silvio Wermelskirchen: Writing – original draft, Investigation, Formal analysis, Data curation, Conceptualization. **Jakob Leonhardi:**

Visualization, Methodology, Formal analysis, Data curation. **Anne-Kathrin Höhn:** Methodology, Investigation, Formal analysis. **Georg Osterhoff:** Validation, Supervision, Resources. **Nikolas Schopow:** Formal analysis, Data curation. **Silke Zimmermann:** Methodology, Formal analysis. **Sebastian Ebel:** Methodology, Investigation. **Gordian Prasse:** Methodology, Investigation. **Jeanette Henkelmann:** Validation, Software. **Timm Denecke:** Validation, Supervision, Resources. **Hans-Jonas Meyer:** Writing – original draft, Formal analysis, Data curation, Conceptualization.

Declaration of competing interest

The authors declare that they have no known competing financial interests or personal relationships that could have appeared to influence the work reported in this paper.

References

[1] S. Mukherjee, Genomics-guided immunotherapy for precision medicine in cancer, Cancer Biother. Radiopharm. 34 (2019) 487–497.
[2] M. Smits, N. Mehra, M. Sedelaar, et al., Molecular biomarkers to guide precision medicine in localized prostate cancer, Expert Rev. Mol. Diagn. 17 (2017) 791–804.
[3] E. Rimondi, G. Rossi, T. Bartalena, et al., Percutaneous CT-guided biopsy of the musculoskeletal system: results of 2027 cases, Eur. J. Radiol. 77 (2011) 34e42.
[4] M.C. Omura, K. Motamedi, S. UyBico, et al., Revisiting CT-guided percutaneous core needle biopsy of musculoskeletal lesions: contributors to biopsy success, AJR Am. J. Roentgenol. 197 (2011) 457e61.
[5] S. Hwang, R.A. Lefkowitz, J. Landa, et al., Percutaneous CT-guided bone biopsy: diagnosis of malignancy in lesions with initially indeterminate biopsy results and CT features associated with diagnostic or indeterminate results, AJR Am. J. Roentgenol. 197 (2011) 1417e25.
[6] A.L. Hryhorczuk, P.J. Strouse, J.S. Biermann, Accuracy of CT-guided percutaneous core needle biopsy for assessment of pediatric musculoskeletal lesions, Pediatr. Radiol. 41 (2011) 848e57.
[7] J.S. Jelinek, M.D. Murphey, J.A. Welker, et al. Diagnosis of primary bone tumors with image-guided percutaneous biopsy: experience with 110 tumors. Radiology 200;223:731e7.
[8] S. Tsukushi, H. Katagiri, H. Nakashima, et al., Application and utility of computed tomography-guided needle biopsy with musculoskeletal lesions, J. Orthop. Sci. 9 (2004) 122e5.
[9] J. Issakov, G. Flusser, Y. Kollender, et al., Computed tomography-guided core needle biopsy for bone and soft tissue tumors, Isr. Med. Assoc. J. 5 (2003) 28e30.
[10] Y. Li, Y. Du, T.Y. Luo, et al., Factors influencing diagnostic yield of CT-guided percutaneous core needle biopsy for bone lesions, Clin. Radiol. 69 (2014) e43–e47.
[11] J.S. Wu, J.D. Goldsmith, P.J. Horwich, et al., Bone and soft-tissue lesions: what factors affect diagnostic yield of image-guided core-needle biopsy? Radiology 248 (2008) 962–970.
[12] C.E. Spritzer, P.D. Afonso, E.N. Vinson, et al., Bone marrow biopsy: RNA isolation with expression profiling in men with metastatic castration-resistant prostate cancer–factors affecting diagnostic success, Radiology 269 (2013) 816–823.
[13] C.H. Suh, S.J. Yun, Diagnostic outcome of image-guided percutaneous core needle biopsy of sclerotic bone lesions: a metaanalysis, AJR Am. J. Roentgenol. 212 (2019) 625–631.
[14] R.E. Coleman, Metastatic bone disease: clinical features, pathophysiology and treatment strategies, Cancer Treat Rev. 27 (2001) 165–176.
[15] R.E. Coleman, R.D. Rubens, The clinical course of bone metastases from breast cancer, Br. J. Cancer 55 (1987) 61–66.
[16] R.E. Coleman, P.I. Croucher, A.R. Padhani, et al., Bone metastases, Nat. Rev. Dis. Primers 6 (2020) 83.
[17] W. Rogers, S. Thulasi Seetha, T.A.G. Refaee, et al., Radiomics: from qualitative to quantitative imaging, Br. J. Radiol. 93 (2020) 20190948.
[18] M.G. Lubner, A.D. Smith, K. Sandrasegaran, et al., CT texture analysis: definitions, applications, biologic correlates, and challenges, Radiographics 37 (2017) 1483–1503.
[19] B.A. Varghese, S.Y. Cen, D.H. Hwang, V.A. Duddalwar, Texture analysis of imaging: what radiologists need to know, AJR Am. J. Roentgenol. 212 (2019) 520–528.
[20] P. Lambin, E. Rios-Velazquez, R. Leijenaar, et al., Radiomics: extracting more information from medical images using advanced feature analysis, Eur. J. Cancer 48 (2012) 441–446.
[21] H.J. Aerts, E.R. Velazquez, R.T. Leijenaar, et al., Decoding tumour phenotype by noninvasive imaging using a quantitative radiomics approach, Nat. Commun. 5 (2014) 4006.
[22] M. Incoronato, M. Aiello, T. Infante, et al., Radiogenomic analysis of oncological data: a technical survey, Int. J. Mol. Sci. 18 (2017) 805.
[23] N. Just, Improving tumour heterogeneity MRI assessment with histograms, Br. J. Cancer 111 (2014) 2205–2213.
[24] R. Donners, N. Fotiadis, I. Figueiredo, et al., Optimising CT-guided biopsies of sclerotic bone lesions in cancer patients, Eur. Radiol. 32 (2022) 6820–6829.
[25] M. Strzelecki, P. Szczypinski, A. Materka, A. Klepaczko, A software tool for automatic classification and segmentation of 2D/3D medical images, Nucl. Instrum. Methods Phys. Res. A 702 (2013) 137–140.
[26] P.M. Szczypiński, M. Strzelecki, A. Materka, A. Klepaczko, MaZda—a software package for image texture analysis, Comput. Methods Prog. Biomed. 94 (2009) 66–76.
[27] H.J. Meyer, S. Schob, A.K. Höhn, A. Surov, MRI texture analysis reflects histopathology parameters in thyroid cancer - a first preliminary study, Transl. Oncol. 10 (2017) 911–916.
[28] J.C. Korte, C. Cardenas, N. Hardcastle, T. Kron, J. Wang, H. Bahig, B. Elgohari, R. Ger, L. Court, C.D. Fuller, S.P. Ng, Radiomics feature stability of open-source software evaluated on apparent diffusion coefficient maps in head and neck cancer, Sci. Rep. 11 (2021) 17633.
[29] A. Zwanenburg, M. Vallières, M.A. Abdalah, et al., The image biomarker standardization initiative: standardized quantitative radiomics for high-throughput image-based phenotyping, Radiology 295 (2) (2020) 328–338.
[30] L. Breiman, Random forests, Machine Learning 45 (2001) 5–32.
[31] B.A. Varghese, D. Hwang, S.Y. Cen, et al., Reliability of CT-based texture features: phantom study, J. Appl. Clin. Med. Phys. 20 (2019) 155–163.
[32] H.J. Meyer, J. Leonhardi, A.K. Höhn, et al., CT texture analysis of pulmonary neuroendocrine tumors-associations with tumor grading and proliferation, J. Clin. Med. 10 (2021) 5571.
[33] S.G. Leffler, F.S. Chew, CT-guided percutaneous biopsy of sclerotic bone lesions: diagnostic yield and accuracy, AJR Am. J. Roentgenol. 172 (1999) 1389–1392.
[34] F.I. Baffour, M.R. Moynagh, P.W. Eiken, et al., Effectiveness and safety of percutaneous CT-guided rib biopsy, J. Vasc. Interv. Radiol. 30 (2019) 82–86.
[35] L. Monfardini, L. Preda, G. Aurilio, et al., CT-guided bone biopsy in cancer patients with suspected bone metastases: retrospective review of 308 procedures, Radiol. Med. 119 (2014) 852–860.